Anellated Hemicyanine Dyes in a Neuron Membrane: Molecular Stark Effect and Optical Voltage Recording

Bernd Kuhn and Peter Fromherz*

Department of Membrane and Neurophysics, Max Planck Institute for Biochemistry, Martinsried/München, Germany

Received: March 6, 2003

The voltage sensitivity of hemicyanine dyes ANNINE-6 and ANNINE-5 with anellated benzene rings and without free CC single and double bonds is studied in Retzius neurons from *Hirudo medicinalis*. For comparison, biaryl hemicyanine BNBIQ and styryl hemicyanines di-4-ANEPBS and RH-421 are investigated. Fluorescence spectra are recorded by an independent variation of the wavelengths of excitation and emission at two defined membrane voltages. With extracellular staining, a positive change in the intracellular voltage shifts all excitation spectra to the blue. That modulation is assigned to a molecular Stark effect that increases in the series RH-421, di-4-ANEPBS, BNBIQ, ANNINE-5, and ANNINE-6 with displacements of elementary charge by 0.24, 0.43, 0.51, 0.65, and 0.81 nm across the membrane. For BNBIQ, ANNINE-5, and ANNINE-6, an almost identical blue shift is observed for the emission that is also assigned to a Stark effect. The ANNINE dyes are the most efficient fluorescent probes of neuronal activity on the basis of a well-defined physical mechanism. The implications with respect to the optical recording of voltage transients are considered.

Introduction

Optical recording of neuronal activity with high spatial and temporal resolution is a crucial prerequisite to the elucidation of the electric function of nerve cells, neuronal networks, and the brain.[1−3] After an initial attempt by Tasaki et al.,[4] in a heroic effort Cohen, Salzberg, and co-workers screened hundreds of organic dyes for their suitability to the optical recording of fast voltage transients in neuron membranes.[5,6] On that foundation, the styryl class of hemicyanine dyes was optimized for the maximum response of their fluorescence change by neuronal activity by Loew et al.[7−9] and Grinvald et al.[10,11] In particular, the dyes di-4-ANEPPS[9] and RH-421[11] (Figure 1) were used in numerous studies with individual nerve cells, neuronal networks, and the brain.

Styryl hemicyanines exhibit striking solvatochromism in bulk solvents of increasing polarity with a blue shift of absorption and a red shift of fluorescence.[12] This symmetrically divergent spectral shift reflects an intramolecular displacement of electrical charge by electronic excitation from the pyridinium moiety toward the aniline moiety of the chromophores (Figure 1). Such a charge displacement was postulated to provide a sound basis for the development of optical probes in nerve cells because of a linear Stark effect.[7] A changing electric field across an asymmetrically stained cell membrane would induce an identical shift in the excitation and emission spectra, leading to a modulated fluorescence intensity for appropriately chosen wavelengths of illumination and detection. However, measurements of excitation and emission spectra in a neuron membrane revealed that the spectral shifts of excitation and emission were not identical and that other changes in the spectral shape played a significant role.[13,14] The mechanism of the voltage sensitivity of the styryl dyes appeared to be rather involved.[15,16]

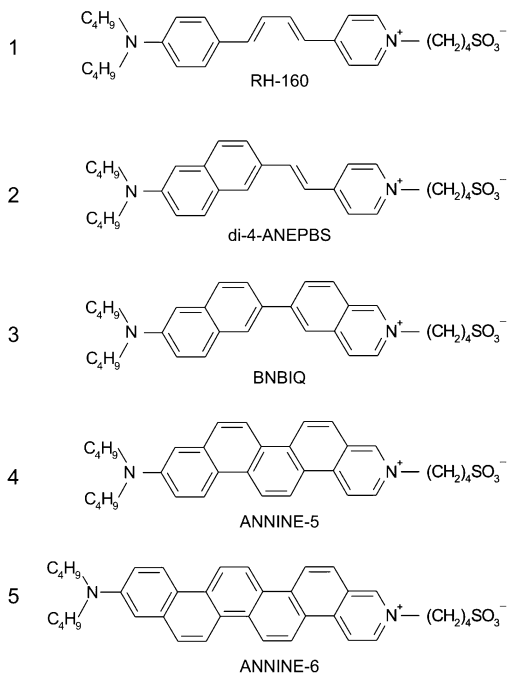

Figure 1. Voltage-sensitive amphiphilic hemicyanine dyes. (1−4) Homologous series with electron-pushing aniline, electron-pulling pyridinium, and two intervening conjugated CC double bonds: styryl dye RH-160 (RH-421 with pentyl substitutents), styryl dye di-4-ANEBPS (di-4-ANEPPS with propylsulfonate), biaryl dye BNBIQ, and anellated hemicyanine dye ANNINE-5. The conformation at the single bonds is matched to the structure of ANNINE-5. (5) Anellated hemicyanine dye ANNINE-6.

There are two effects that may interfere with a Stark-effect mechanism: (i) The styryl chromophores are not rigid. Electronic excitation gives rise to photoisomerism of CC double bonds and to photorotamerism of CC single bonds.[17] Both

* Corresponding author. E-mail: fromherz@biochem.mpg.de. Phone: +49 89 8578 2820. Fax: +49 89 8578 2822.

10.1021/jp0345811 CCC: $25.00
Published on Web 07/02/2003

processes may be related to an intramolecular displacement of an electrical charge shift and may be affected by an electrical field. In particular, rotamerism was shown to lead to a twisted internal charge-transfer (TICT) state with a reduced fluorescence quantum yield.[18] (ii) The styryl chromophores are not immobilized in a membrane. Their amphiphilic structure guarantees an accumulation at the membrane surface[19] and some alignment along the membrane normal.[20,21] But a changing electric field may affect the position or inclination of the chromophores, and the inhomogeneous environment at the membrane surface may give rise to a field-induced solvatochromic effect.[16,22]

In earlier work, the dynamics of the hemicyanines was simplified by incorporating the CC double bonds in aromatic rings.[23] Biaryl dye BNBIQ (diButyl-Naphthylamino-Butyl-sulfonato-IsoQuinolinium) (Figure 1) exhibited symmetrically divergent solvatochromism that was distinctly stronger than with the homologous di-4-ANEPBS and RH-421.[12] Correspondingly, its voltage sensitivity in a neuron membrane was higher.[14] In a second stage, the free CC single bonds were also eliminated, with chromophores consisting of anellated benzene rings.[24] The solvatochromism of anellated hemicyanines ANNINE-5 and ANNINE-6 (Figure 1) was also significantly enhanced compared to that of the styryl dyes, indicating a large intramolecular displacement of electric charge.

In the present paper, we describe the voltage sensitivity of anellated hemicyanines ANNINE-6 and ANNINE-5 and, for comparison, that of BNBIQ, di-4-ANEPBS, and RH-421. Two-dimensional fluorescence spectra of excitation and emission are measured in leech neurons at defined membrane voltages. The voltage-induced changes in fluorescence are parametrized in terms of changes in spectral parameters. We find that the ANNINE dyes are far more voltage-sensitive than the classical styryl dyes and that their sensitivity can be assigned almost completely to an identical spectral shift of excitation and emission that is caused by a molecular Stark effect.

Materials and Methods

Dyes. Styryl dye RH-421[11] was obtained from Molecular Probes (Eugene, OR). Styryl dye di-4-ANEPBS[9] and Biaryl dye BNBIQ[23] were synthesized by Gerd Hübener. The syntheses of dyes ANNINE-5 and ANNINE-6 are described in ref 24.

Neurons. Ganglia of the leech *Hirudo medicinalis* (Moser, Schorndorf, Germany) were dissected and pinned on a Sylgard-coated dish in Leibowitz-15 medium (L-5520, Sigma, Deisenhofen) with 5 mg/mL glucose, 0.3 mg/mL glutamine, and 3 μg/mL gentamycin sulfate (G-3632, Sigma).[25] After opening the tissue capsules, we incubated the ganglia in dispase/collagenase (Boehringer, Mannheim, 2 mg/mL L-15 medium) for 1 h at room temperature. Retzius cells (soma diameter 60−90 μm) were dissociated by aspiration into a fire-polished micropipet and washed with Leibowitz-15 medium.[25] The cells were seeded on an uncoated glass cover slip in a silicone chamber (Flexiperm-mikro 12, Vivascience AG, Hannover, Germany) with Leibowitz-15 medium and 2.5% fetal bovine serum (10106, Gibco, Eggenstein) and kept for 1 or 2 days at 20 °C.

Staining. The dyes were solubilized in Leibowitz-15 medium with sodium cholate (Sigma, St. Louis, MO).[26] We used 4.3 mM RH-421 with 10 mM cholate, 4.3 mM di-4-ANEPBS with 10mM cholate, 10 mM BNBIQ with 10 mM cholate, 1 mM ANNINE-5 with 23 mM cholate, and 1 mM ANNINE-6 with 25 mM cholate. After centrifugation, the staining solutions were added to the culture chambers with the neurons in a volume ratio of 1:1000 30 min before patching. The solubility of the dyes in water decreases in the series RH-421, di-4-ANEPBS, BNBIQ, ANNINE-5, and ANNINE-6. Correspondingly, the fluorescence intensity of cells stained with RH-421 and di-4-ANEPBS dropped after exchanging the medium with a dye-free solution because of desorption from the cells, whereas the intensity with ANNINE-5 and ANNINE-6 remained constant for at least 1.5 h. With respect to bleaching and phototoxicity, we did not observe significant differences under comparable conditions of staining and illumination.

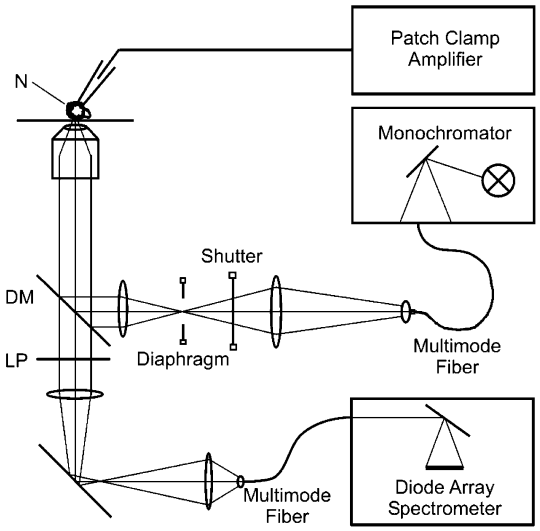

Figure 2. Experimental setup. A nerve cell (N) stained with a voltage-sensitive dye is kept at a defined intracellular voltage by a micropipet using a patch-clamp amplifier. The cell is illuminated in a microscope through the monochromator, shutter, dichroic mirror (DM), and objective. The fluorescence passes the dichroic mirror and a long-pass filter (LP) and is detected by a diode array spectrometer. The complete fluorescence spectrum is recorded for a wide range of excitation wavelengths at two different transmembrane voltages.

Electrophysiology. Patch pipets with a tip diameter of 5−10 μm were made from microhaematocrite tubes (Assistent, Karl Hecht, Sondheim/Rhön, Germany) using an all-purpose puller (DMZ-Universal Puller, Zeitz-Instrumente, Augsburg, Germany). They were filled with 140 mM KCl, 1.5 mM $MgCl_2$, 10 mM Hepes, and 10 mM EGTA, pH 7.3. The resistance of the pipets was around 0.4 MΩ. The pipets with Ag/AgCl electrodes were connected to a single electrode patch-clamp amplifier (SEC-10L, npi, Tamm, Germany). The patching of Retzius cells led to a seal resistance of about 500 MΩ. Whole cell contact[27] was achieved by breaking the membrane with suction using a water-jet vacuum pump. The bath was held at ground potential with a Ag/AgCl electrode. We kept the cells at an intracellular voltage of $V_M = -40$ mV. The fluorescence spectra were measured at a hyperpolarized voltage of $V_M = -70$ mV and a depolarized voltage of about $V_M = 10$ mV.

Optical Setup. The spectrometer is sketched in Figure 2. It is built on the basis of an inverted microscope (Axiovert 35, Zeiss, Oberkochen, Germany) with a high numerical aperture oil-immersion objective (Neofluar 100×/1.3 oil). The light of a 75-W xenon short arc lamp (Ushio, Hyogo, Japan) is spectrally resolved (resolution 16 nm) by a grating monochromator (J&M, Aalen, Germany). It is fed into the microscope with an optical multimode fiber (diameter 1.2 mm) and collimating optics (J&M). Nerve cells are illuminated through a dichroic mirror (AHF analysentechnik, Tübingen, Germany) with a splitting wavelength of 520 nm for RH-421, di-4-ANEPPS, BNBIQ, and ANNINE-6 and 460 nm for ANNINE-5. The illumination is controlled by a shutter and a field diaphragm. The light emitted

by the stained cell is collected by the objective. It passes through the dichroic mirror and a long-pass filter (AHF analysentechnik, Tübingen) with a cutoff at 520 nm for RH-421, di-4-ANEPBS, BNBIQ, and ANNINE-6 and 470 nm for ANNINE-5 and is guided by an optical fiber (0.6 mm) to a diode array spectrometer (J&M) with a spectral range from 307 to 1135 nm at a resolution of 3.1 nm.

Calibrated Fluorescence Spectra. To derive molecular parameters from the experimental data, the 2D spectra of excitation and emission were calibrated. The number of excitations per unit time in a membrane area A_{mem} with n_{dye} molecules per unit area is $A_{mem}n_{dye}\epsilon(\lambda_{ex})I_\lambda^{ill}(\lambda_{ex})\Delta\lambda_{ex}$ with the molecular cross section of absorption $\epsilon(\lambda_{ex})$ and the quantum intensity of illumination per wavelength interval $I_\lambda^{ill}(\lambda_{ex})$ at a bandwidth $\Delta\lambda_{ex}$. The number of detected quanta per unit time $P(\lambda_{ex}, \lambda_{em})$ is given by eq 1 with the quantum yield Φ_{em}, the normalized quantum spectrum of fluorescence per wavelength interval $f_\lambda(\lambda_{em})$, and the efficiency $T^{rec}(\lambda_{em})$ and bandwidth $\Delta\lambda_{em}$ of the recording system.

$$P(\lambda_{ex},\lambda_{em}) = A_{mem}n_{dye}I_\lambda^{ill}(\lambda_{ex})\Delta\lambda_{ex}\epsilon(\lambda_{ex})\Phi_{em}f_\lambda(\lambda_{em})T^{rec}(\lambda_{em})\Delta\lambda_{em} \quad (1)$$

We obtain a 2D fluorescence spectrum that is defined by molecular parameters when we divide eq 1 by the number of dye molecules $A_{mem}n_{dye}$ and by the spectra and bandwidths of illumination $I_\lambda^{ill}(\lambda_{ex})\Delta\lambda_{ex}$ and recording $T^{rec}(\lambda_{em})\Delta\lambda_{em}$. The resulting fluorescence spectrum of excitation and emission per unit wavenumber of emission $F_{\bar\nu}(\bar\nu_{ex},\bar\nu_{em}) = \epsilon(\bar\nu_{ex})\Phi_{em}f_{\bar\nu}(\bar\nu_{em})$ is given by eq 2, considering the relations $f_{\bar\nu}(\bar\nu_{em}) = \lambda_{em}^2 f_\lambda(\lambda_{em})$ and $\epsilon(\bar\nu_{ex}) = \epsilon(\lambda_{ex})$.

$$F_{\bar\nu}(\bar\nu_{ex},\bar\nu_{em}) = \frac{\lambda_{em}^2}{A_{mem}n_{dye}I_\lambda^{ill}(\lambda_{ex})\Delta\lambda_{ex}T^{rec}(\lambda_{em})\Delta\lambda_{em}}P(\lambda_{ex},\lambda_{em}) \quad (2)$$

$T^{rec}(\lambda_{em})\Delta\lambda_{em}$ is obtained up to an arbitrary factor by calibrating the recording system (objective, dichroic mirror, long-pass filter, 0.6-mm fiber optics, monochromator, and diode array). We place a standard lamp (OL245M, Optronic Laboratories, Orlando, FL) with a known quantum spectrum $I_\lambda^{cal}(\lambda)$ on the microscope and measure the response $P^{cal}(\lambda) = I_\lambda^{cal}(\lambda)T^{rec}(\lambda_{em})\Delta\lambda_{em}$ of the photodiode array. We probe the illumination (Xe lamp, monochromator, optical fiber, broadening optics, dichroic mirror, and objective) with a calibrated detector of efficiency $T^{cal}(\lambda)$ and bandwidth $\Delta\lambda$. For that purpose, we use part of our recording system—the 0.6 nm optical fiber with monochromator and diode array—that is again calibrated by illuminating the fiber end with the standard lamp. With the fiber end on the microscope, we measure $P^{ill}(\lambda) = I_\lambda^{ill}(\lambda_{ex}^{nom},\lambda)T^{cal}(\lambda)\Delta\lambda$ for each λ_{ex}^{nom} set at the monochromator. The resulting illumination spectra $I_\lambda^{ill}(\lambda_{ex}^{nom},\lambda)$ are fitted with Gaussians with a maximum defining the excitation wavelenth λ_{ex} and an integral that represents the intensity $I_\lambda^{ill}(\lambda_{ex})\Delta\lambda_{ex}$ up to a constant factor.

Protocol. The measurements were started 30 min after staining. Under a voltage clamp, the voltage-sensitive fluorescence is investigated with the following protocol: (1) opening of the shutter, (2) selection of an excitation wavelength λ_{ex}, (3) after a delay of 100 ms, hyperpolarization of the cell to $V_M = -70$ mV, (4) recording of a complete emission spectrum in the range of $\lambda_{em} = 510-833$ nm for RH-421, di-4-ANEPBS, BNBIQ, and ANNINE-6 and $\lambda_{em} = 460-833$ nm for ANNINE-5 with an integration time of 200 ms, (5) after a delay of 100 ms, depolarization to about $V_M = 10$ mV, (6) recording of two complete emission spectra, (7) after a delay of 100 ms, hyperpolarization to $V_M = -70$ mV, (8) recording another complete emission spectrum, and (9) closing the shutter. Steps 2−8 are repeated for various wavelengths of excitation in the range of $\lambda_{ex} = 360-510$ nm for RH-421, di-4-ANEPBS, BNBIQ, and ANNINE-6 and $\lambda_{ex} = 360-460$ nm for ANNINE-5 at a step width of 5 nm. At each excitation wavelength, the two spectra of the hyperpolarized cell as well as the two spectra of the depolarized cell are averaged to obtain spectra $P(\lambda_{ex},\lambda_{em})$ at the two voltages. The 2D fluorescence spectra $F_{\bar\nu}(\bar\nu_{ex},\bar\nu_{em})$ are computed according to eq 2 up to a constant factor using the spectra $I_\lambda^{ill}(\lambda_{ex})\Delta\lambda_{ex}$ and $T^{rec}(\lambda_{em})\Delta\lambda_{em}$ given by calibration. At the hyperpolarized voltage, the spectrum is scaled to its maximum as $F_{\bar\nu}^{hyp}/F_{\bar\nu}^{hyp,max}$. At the depolarized voltage, the spectrum is scaled by the same factor as $F_{\bar\nu}^{dep}/F_{\bar\nu}^{hyp,max}$.

Results

Two-Dimensional Spectra. The relative fluorescence spectra per wavenumber interval of emission $F_{\bar\nu}(\bar\nu_{ex},\bar\nu_{em})/F_{\bar\nu}^{max}$ in Retzius neurons at a voltage $V_M = -70$ mV are plotted in the left column of Figure 3 for RH-421, di-4-ANEPBS, BNBIQ, ANNINE-5, and ANNINE-6. They are limited at the red end of excitation and the blue end of emission by the dichroic mirror of the microspectrometer. The maxima reflect the position of the upward and downward vibroelectronic transitions between the S_0 and S_1 states of the dyes. They are shifted to higher wavenumbers of excitation and emission in the homologous series RH-421, di-4-ANEPBS, BNBIQ, and ANNINE-5 and also in ANNINE-6. With respect to excitation, a second band appears in the ANNINEs at high wavenumbers because of the S_0/S_2 transition.

One-Dimensional Spectra. To study the interdependence of excitation and emission, we consider emission spectra per wavenumber of emission $F_{\bar\nu}(\bar\nu_{em})$ at various wavenumbers of excitation $\bar\nu_{ex}$ and excitation spectra $F_{\bar\nu}(\bar\nu_{ex})$ per wavenumber of emission for various wavenumbers of emission $\bar\nu_{em}$ in the 2D spectra. These 1D spectra are fitted by log-normal functions[28] according to eq 3 with an amplitude $F_{\bar\nu}^{max}$, a spectral maximum $\bar\nu^{max}$, a spectral width W, and a spectral asymmetry b, excluding the contribution of the S_0/S_2 transition.

$$\frac{F_{\bar\nu}(\bar\nu)}{F_{\bar\nu}^{max}} = \exp\left\{-\frac{\ln^2[1 + 2b(\bar\nu - \bar\nu^{max})/W]}{b^2/\ln 2}\right\} \quad (3)$$

Figure 4 shows the parameters of the emission spectra $\bar\nu_{em}^{max}$, W_{em}, and b_{em} as a function of the excitation wavenumber $\bar\nu_{ex}$ and the parameters of the excitation spectra $\bar\nu_{ex}^{max}$, W_{ex}, and b_{ex} as a function of the emission wavenumber $\bar\nu_{em}$. The maximum of excitation is shifted to the blue at high wavenumbers of emission, and the maximum of emission is shifted to the blue for higher wavennumbers of excitation. Such effects are expected for hemicyanine dyes when the solvent shell is incompletely relaxed in the excited state.[18] However, these shifts of the spectral maxima as well as all other changes of spectral width and spectral asymmetry displayed in Figure 4 are rather small compared with the width of the spectra and the difference in excitation and emission maxima. Considering these observations with the 1D spectra, we use in the following evaluation of the 2D spectra the approximation that excitation and emission processes are independent of each other.

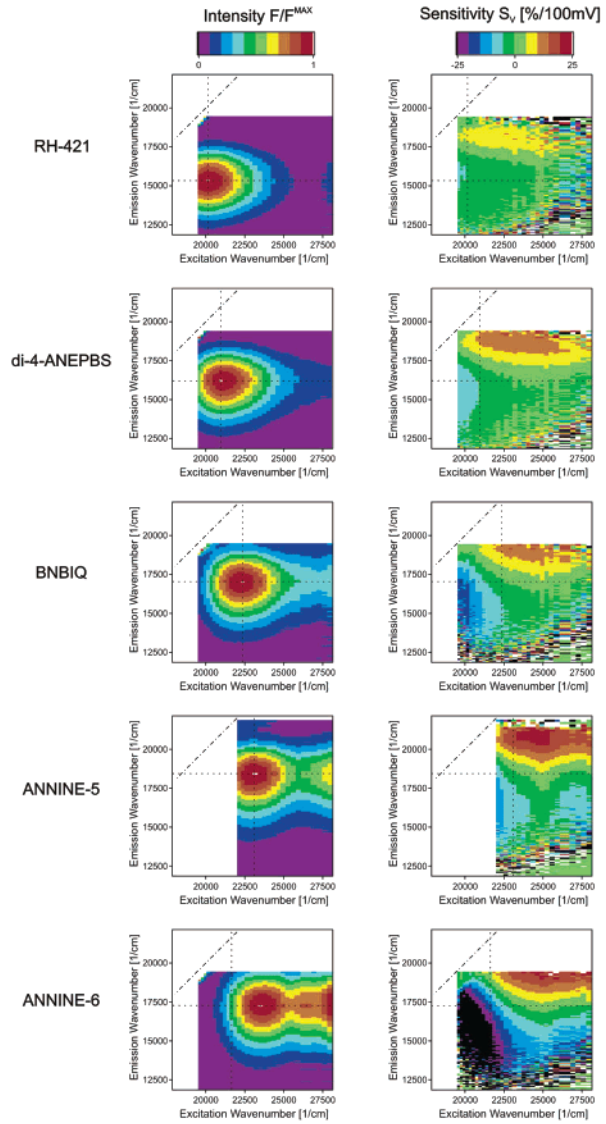

Figure 3. Experimental 2D fluorescence spectra. Left column: Color-coded relative fluorescence intensity $F_{\bar{\nu}}(\bar{\nu}_{ex},\bar{\nu}_{em})/F_{\bar{\nu}}^{max}$ in Retzius cells at a voltage of $V_M = -70$ mV as a function of the wavenumbers of excitation (abscissa) and emission (ordinate). Right column: Color-coded voltage sensitivity of fluorescence $S_V(\bar{\nu}_{ex},\bar{\nu}_{em}) = \Delta F_{\bar{\nu}} F_{\bar{\nu}} \Delta V_M$. The diagonal lines mark equal wavenumbers of excitation and emission. The dotted vertical and horizontal lines indicate 1D spectra of excitation and emission. They are chosen through the 2D maxima with the exception of ANNINE-6, where the excitation is chosen in the red to avoid a contribution of the S_0/S_2 transition.

Fit of 2D Spectra. To attain a well-defined parametrization of the fluorescence spectra, we fit the normalized 2D spectra $F_{\bar{\nu}}(\bar{\nu}_{ex},\bar{\nu}_{em})/F_{\bar{\nu}}^{max}$ shown in the left column of Figure 3 to the products of two log-normal spectra according to eq 4.

$$\frac{F_{\bar{\nu}}(\bar{\nu}_{ex},\bar{\nu}_{em})}{F_{\bar{\nu}}^{max}} = \exp\left\{-\frac{\ln^2[1+2b_{ex}(\bar{\nu}-\bar{\nu}_{ex}^{max})/W_{ex}]}{b_{ex}^2/\ln 2}\right\} \times \exp\left\{-\frac{\ln^2[1+2b_{em}(\bar{\nu}-\bar{\nu}_{em}^{max})/W_{em}]}{b_{em}^2/\ln 2}\right\} \quad (4)$$

Considering $F_{\bar{\nu}}(\bar{\nu}_{ex},\bar{\nu}_{em}) = \epsilon(\bar{\nu}_{ex})\Phi_{em} f_{\bar{\nu}}(\bar{\nu}_{em})$ with the cross section of absorption $\epsilon(\bar{\nu}_{ex})$, the quantum yield Φ_{em}, and the normalized quantum spectrum of emission $f_{\bar{\nu}}(\bar{\nu}_{em})$, the product function of eq 4 accounts for the spectral shape of absorption and emission. The five sets of the six spectral parameters are summarized in Table 1, and the fitted 2D spectra are displayed in the left column of Figure 5. We note a distinct asymmetry of the 2D spectra, in particular, for ANNINE-5 and ANNINE-6 with steep slopes toward the red in excitation and toward the blue in emission. To illustrate the quality of the fit, we check 1D sections along the axes of excitation and emission. The upper graphs of Figure 6 show the data and the fit function. The good agreement, except for high wavenumbers of excitation where the contribution of the S_0/S_2 transition is significant, confirms the validity of the approach. Also, the 1D spectra exhibit steep slopes in the red of the excitation band and in the blue of the emission band.

TABLE 1: Spectral Parameters of Excitation and Emission Spectra for the S_0/S_1 Transition of Hemicyanine Dyes in Neuron Membranes[a]

	$\bar{\nu}_{ex}^{max}$ [cm^{-1}]	$\bar{\nu}_{em}^{max}$ [cm^{-1}]	W_{ex} [cm^{-1}]	W_{em} [cm^{-1}]	b_{ex}	b_{em}
RH-421	20 249	15 417	4185	3239	0.340	−0.025
di-4-ANEPBS	21 199	16 390	4176	3292	0.404	−0.226
BNBIQ	22 298	17 125	4327	3471	0.413	−0.219
ANNINE-5	23 155	18 419	3986	3427	0.492	−0.289
ANNINE-6	23 673	17 456	4326	3688	0.321	−0.206

[a] Spectral maxima $\bar{\nu}_{ex}^{max}$ and $\bar{\nu}_{em}^{max}$, spectral widths W_{ex} and W_{em}, and spectral asymmetries b_{ex} and b_{em} are obtained from 2D fluorescence spectra at a voltage of $V_M = -70$ mV by fitting the products of two log-normal functions.

Voltage Sensitivity. The spectrum of voltage sensitivity $S_V(\bar{\nu}_{ex},\bar{\nu}_{em})$ is defined as the relative change in fluorescence intensity per change in membrane voltage according to eq 5.

$$S_V(\bar{\nu}_{ex},\bar{\nu}_{em}) = \frac{\Delta F_{\bar{\nu}}(\bar{\nu}_{ex},\bar{\nu}_{em})}{F_{\bar{\nu}}(\bar{\nu}_{ex},\bar{\nu}_{em})}\frac{1}{\Delta V_M} \quad (5)$$

We obtain it by subtracting the relative spectrum $F_{\bar{\nu}}^{hyp}/F_{\bar{\nu}}^{hyp,max}$ at a hyperpolarized voltage from the scaled spectrum $F_{\bar{\nu}}^{dep}/F_{\bar{\nu}}^{hyp,max}$ at a depolarized voltage and dividing by $F_{\bar{\nu}}^{hyp}/F_{\bar{\nu}}^{hyp,max}$ and the voltage difference ΔV_M. The results, scaled to a voltage $\Delta V_M = 100$ mV, are shown in the right column of Figure 3. All sensitivity spectra exhibit two regions: at high wavenumbers of excitation and emission, the fluorescence is enhanced; at low wavenumbers, the fluorescence is reduced. The magnitude of this effect increases in the homologous series RH-421, di-4-ANEPBS, BNBIQ, and ANNINE-5 and also in ANNINE-6. Within the limited spectral window of the measurements, the sensitivity is in the range of 10%/100 mV for RH-421, 15%/100 mV for di-4-ANEPPS, 200/100 mV for BNBIQ, and 25/100 mV for ANNINE-5 and ANNINE-6.

Parametrized Voltage Sensitivity. A parametrization of voltage sensitivity is achieved by fitting the scaled spectra $F_{\bar{\nu}}^{dep}/F_{\bar{\nu}}^{hyp,max}$ and $F_{\bar{\nu}}^{hyp}/F_{\bar{\nu}}^{hyp,max}$ at the two voltages to the products of log-normal functions according to eq 4. The resulting differences in spectral parameters $\Delta\bar{\nu}_{ex}^{max}$, $\Delta\bar{\nu}_{em}^{max}$, ΔW_{ex}, ΔW_{em}, Δb_{ex}, Δb_{em}, and $\Delta F_{\bar{\nu}}^{max}$ are small for all dyes. For that reason, we can assume that the changes in the spectra are linear with respect to changes in the spectral parameters, and we are allowed to scale the parameter changes to a standard voltage change of $\Delta V_M = 100$ mV, which is typical for neuronal excitation. The resulting differences are shown in Table 2.

Using the fit parameters from Tables 1 and 2, we reconstruct the sensitivity spectra $S_V(\bar{\nu}_{ex},\bar{\nu}_{em})$ according to eq 5. The results are displayed in the central column of Figure 5 in a range where the relative change in intensity is above 10%. For ANNINE-6, ANNINE-5, and BNBIQ, the fitted sensitivity spectra exhibit a distinct enhancement and reduction of fluorescence at high and

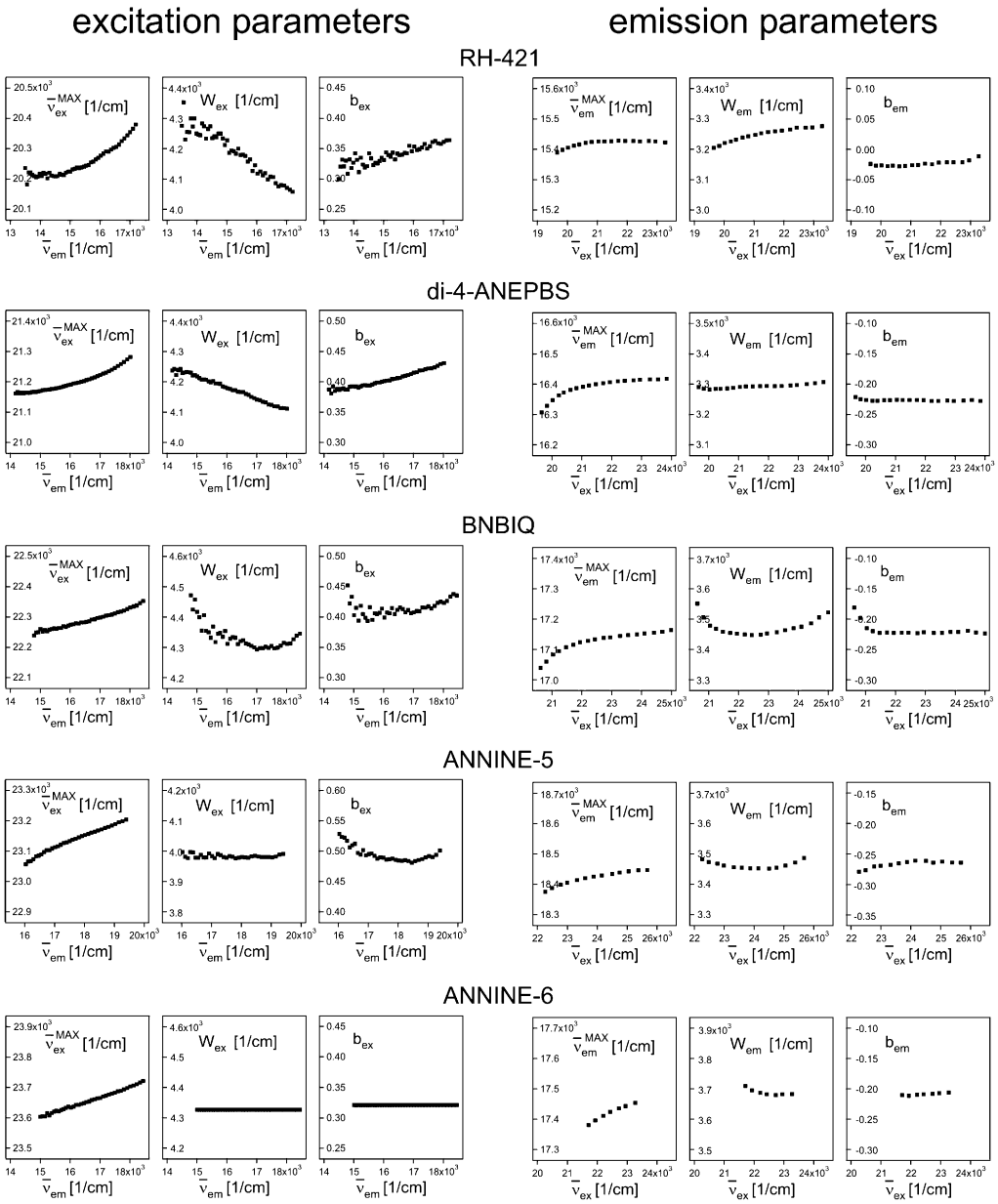

Figure 4. Mutual dependence of excitation and emission spectra. Left: Spectral parameters of the excitation spectra (maximum $\bar{\nu}_{ex}^{max}$, width W_{ex}, asymmetry b_{ex}) as a function of emission wavenumber $\bar{\nu}_{em}$. Right: Spectral parameters of the emission spectra (maximum $\bar{\nu}_{em}^{max}$, width W_{em}, asymmetry b_{em}) as a function of excitation wavenumber $\bar{\nu}_{ex}$.

low wavenumbers, respectively. In particular, we note the steep increase in negative sensitivity with decreasing wavenumber of excitation in the red corner of the 2D spectrum and the steep increase in positive sensitivity with increasing wavenumber of emission in the blue corner of the 2D spectrum. For the two styryl dyes, the sensitivity spectra are more involved.

To illustrate the quality of the sensitivity spectra $S_V(\bar{\nu}_{ex},\bar{\nu}_{em})$ reconstructed from the fit of the 2D spectra at two voltages, we select 1D spectra $S_V(\bar{\nu}_{ex})$ and $S_V(\bar{\nu}_{em})$ across the sensitivity data (Figure 3) and across the fitted spectra (Figure 5). They are shown in Figure 6 and exhibit good agreement, except for high excitation wavenumbers where the S_0/S_2 transition contributes and at low emission wavenumbers where the intensity is modest.

Discussion

Voltage Sensitivity. An electric field across a cell membrane may in principle affect the electronic structure of a bound chromophore, its vibroelectronic coupling, and its interaction with the matrix. It may change the electronic 00 transition energy, the Franck−Condon factors of excitation and emission, the transition dipole moments, and the radiationless deactivation channels. As a result, the 2D fluorescence spectrum $F_{\bar{\nu}}(\bar{\nu}_{ex},\bar{\nu}_{em}) = \epsilon(\bar{\nu}_{ex})\Phi_{em}\, f_{\bar{\nu}}(\bar{\nu}_{em})$ may be modulated through the absorption spectrum $\epsilon(\bar{\nu}_{ex})$, the quantum yield of emission Φ_{em}, and the normalized quantum spectrum of emission $f_{\bar{\nu}}(\bar{\nu}_{em})$. The sensitivity spectrum defined by eq 5 reflects changes in all of these molecular parameters according to eq 6.

$$S_V(\bar{\nu}_{ex},\bar{\nu}_{em}) = \frac{1}{\epsilon(\bar{\nu}_{ex})}\frac{\Delta\epsilon(\bar{\nu}_{ex})}{\Delta V_M} + \frac{1}{\Phi_{em}}\frac{\Delta\Phi_{em}}{\Delta V_M} + \frac{1}{f_{\bar{\nu}}(\bar{\nu}_{em})}\frac{\Delta f_{\bar{\nu}}(\bar{\nu}_{em})}{\Delta V_M} \quad (6)$$

In fact, when we fit the 2D fluorescence spectra at two voltages to products of log-normal functions, we find that the joined amplitude $F_{\bar{\nu}}^{max}$ and all spectral parameters of excitation

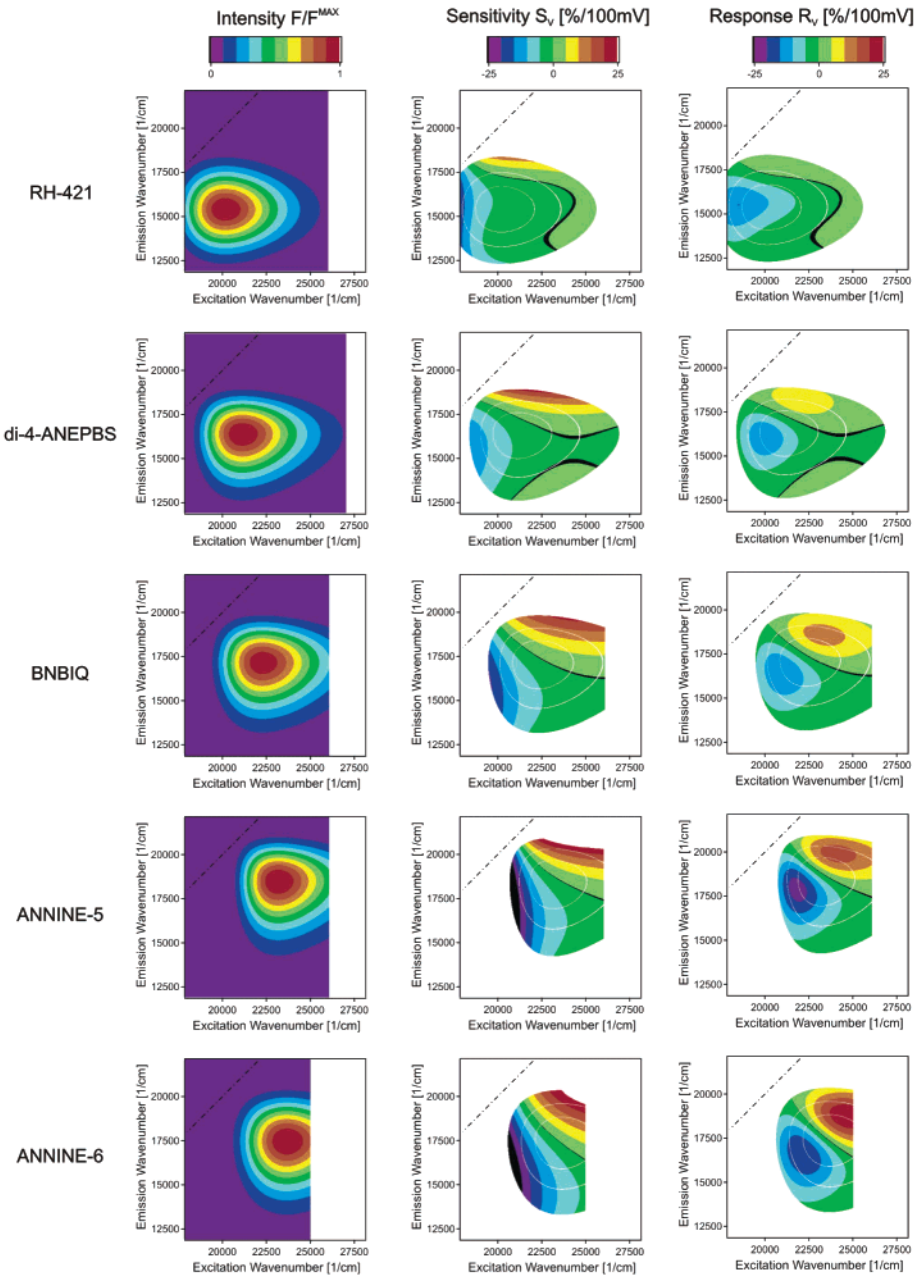

Figure 5. Two-dimensional fluorescence spectra parametrized by the product of log-normal functions. Left column: color-coded relative fluorescence spectra $F_{\bar{\nu}}(\bar{\nu}_{ex},\bar{\nu}_{em})/F_{\bar{\nu}}^{max}$ at $V_M = -70$ mV. Central column: color-coded sensitivity spectra $S_V(\bar{\nu}_{ex},\bar{\nu}_{em}) = \Delta F_{\bar{\nu}}/F_{\bar{\nu}}\Delta V_M$ in a range where $F_{\bar{\nu}}/F_{\bar{\nu}}^{max} > 0.1$ and where the S_0/S_2 transition plays a negligible role. Right column: color-coded relative response spectra $R_V = \Delta F_{\bar{\nu}}/F_{\bar{\nu}}^{max}\Delta V_M$. The diagonals mark equal wavenumbers of excitation and emission. White lines in the sensitivity and response spectra indicate intensity levels $F_{\bar{\nu}}/F_{\bar{\nu}}^{max} = 0.33$ and $F_{\bar{\nu}}/F_{\bar{\nu}}^{max} = 0.67$. Black lines mark the change in sign of sensitivity and response.

$\bar{\nu}_{ex}^{max}$, W_{ex}, and b_{ex} and of emission $\bar{\nu}_{em}^{max}$, W_{em}, and b_{em} are modified by an electric field as summarized in Table 2. An assignment of these parameter changes to molecular mechanisms, however, is difficult (e.g., spectral shifts $\Delta\bar{\nu}_{ex}^{max}$ and $\Delta\bar{\nu}_{em}^{max}$ may arise not only from a change in the electronic 00 energy and amplitude changes $\Delta F_{\bar{\nu}}^{max}$ not only from a changed fluorescence quantum yield, but in both cases, changes in spectral shape contribute, too). It is also a problem that parameter changes $\Delta\bar{\nu}_{ex}^{max}$, $\Delta\bar{\nu}_{em}^{max}$, ΔW_{ex}, ΔW_{em}, Δb_{ex}, Δb_{em}, and $\Delta F_{\bar{\nu}}^{max}$ are derived from a small difference between two spectra, a procedure that implies a large error. For both reasons, we do not attempt to provide a detailed mechanistic interpretation of voltage sensitivity. We consider only one aspect—the possible contribution of a molecular Stark effect.

Electrochromism of Excitation. A typical feature of the voltage sensitivity of all of the hemicyanines considered is a blue shift $\Delta\bar{\nu}_{ex}^{max}$ of all excitation spectra induced by a positive change ΔV_M in the membrane voltage (Table 2). This blue shift increases in the homologous series RH-421, di-4-ANEPBS, BNBIQ, ANNINE-5 and also in ANNINE-6. To confirm the significance of this observation, we repeat the evaluation of the spectral data in terms of a product of log-normal functions (eq 4) with five parameters at constant spectral asymmetries b_{ex} and b_{em} and also with three parameters at constant asymmetries and constant spectral widths W_{ex} and W_{em}. The resulting spectral shifts are summarized in Table 3. Apparently, the systematic blue shift of excitation is rather insensitive to the fitting procedure.

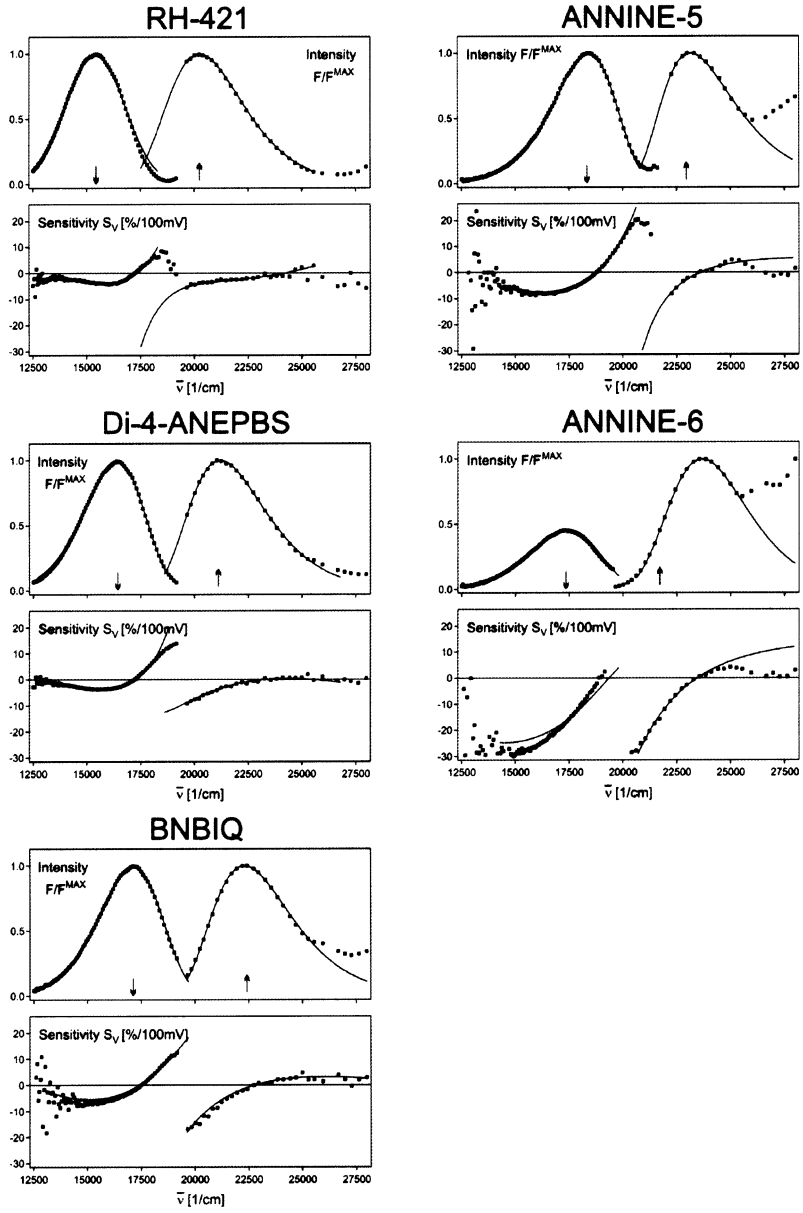

Figure 6. One-dimensional spectra of fluorescence and voltage sensitivity. Upper plots: spectra of the relative intensity of emission $F_{\bar{\nu}}(\bar{\nu}_{em})/F_{\bar{\nu}}^{max}$ and excitation $F_{\bar{\nu}}(\bar{\nu}_{ex})/F_{\bar{\nu}}^{max}$ across the 2D spectra as indicated in Figure 3. Lower plots: sensitivity spectra of emission $S_V(\bar{\nu}_{em})$ and excitation $S_V(\bar{\nu}_{ex})$. The drawn lines are 1D sections of the fit with the product of two log-normal functions taken from Figure 5. The wavenumbers of excitation and emission are marked by arrows.

TABLE 2: Voltage Sensitivity of the Spectral Parameters of Excitation and Emission for the S_0/S_1 Transition of the Hemicyanine Dyes in a Neuron Membrane[a]

	$\Delta\bar{\nu}_{ex}^{max}$ [cm^{-1}]	$\Delta\bar{\nu}_{em}^{max}$ [cm^{-1}]	ΔW_{ex} [cm^{-1}]	ΔW_{em} [cm^{-1}]	Δb_{ex}	Δb_{em}	$\Delta F_{\bar{\nu}}^{max}$
RH-421	47	−18	−49	54	0.022	0.029	−0.039
di-4-ANEPBS	90	45	38	83	−0.024	0.006	−0.033
BNBIQ	103	99	8	24	−0.009	−0.014	−0.011
ANNINE-5	132	132	12	20	0.002	−0.016	−0.015
ANNINE-6	163	170		−19		0.022	0.018

[a] Two-dimensional spectra of fluorescence are fitted with products of two log-normal functions at two different voltages. The changes in the spectral parameters—of the maxima $\Delta\bar{\nu}_{ex}^{max}$ and $\Delta\bar{\nu}_{em}^{max}$, of the widths ΔW_{ex} and ΔW_{em}, of the asymmetries Δb_{ex} and Δb_{em}, and of the amplitude $\Delta F_{\bar{\nu}}^{max}$—are scaled to a voltage change of $\Delta V_M = 100$ mV. For ANNINE-6, the width and asymmetry of excitation was held constant because of an overlap with S_0/S_2 excitation.

We assign the blue shift of excitation to a molecular Stark effect of the membrane-bound chromophores.[29−32] Because of their amphiphilic structure, the hemicyanines may be expected to be bound to the surface of the neuron membrane with a distinct orientation.[20,21] In that case, an intramolecular charge displacement $\Delta_i\mu_{EG}$ by electronic excitation from the pyridinium to the aniline moiety is directed against a change $\Delta E = \Delta V_M/d_M$ of the average electrical field in a membrane of thickness d_M as induced by a positive change ΔV_M of the membrane voltage. The expected blue shift is expressed by eq 7 with a projection

TABLE 3: Spectral Shifts of Excitation and Emission by a Voltage Change of $\Delta V_M = 100$ mV[a]

	$\Delta\bar{\nu}_{ex}^{max}$ [cm^{-1}]			$\Delta\bar{\nu}_{em}^{max}$ [cm^{-1}]		
	7 param	5 param	3 param	7 param	5 param	3 param
RH-421	47	46	47	−18	−3	−6
di-4-ANEPBS	90	78	78	45	43	42
BNBIQ	103	97	96	99	91	91
ANNINE-5	132	132	134	132	123	123
ANNINE-6	163	163	163	170	159	159

[a] Two-dimensional fluorescence spectra at two different voltages are fitted with products of two lognormal functions. The changes in the spectral maxima $\Delta\bar{\nu}_{ex}^{max}$ and $\Delta\bar{\nu}_{em}^{max}$ are shown for (i) a fit with seven changing spectral parameters (maxima, widths, spectral asymmetries, amplitude), (ii) a fit with five changing spectral parameters (maxima, widths, amplitude), and (iii) a fit with three changing spectral parameters (maxima, amplitude).

cos ϑ of charge displacement on the membrane normal (Planck's constant h, velocity of light c).

$$hc\Delta\bar{\nu}_{ex}^{max} = \Delta\mu_{EG}\Delta E\cos\vartheta \qquad (7)$$

From the experimental shifts $\Delta\bar{\nu}_{ex}^{max}$, we estimate the charge displacement $\Delta\mu_{EG}\cos\vartheta$ along the membrane normal for $\Delta V_M = 100$ mV and $d_M = 4$ nm. Considering the fit with seven parameters (Table 2), we obtain for RH-421, di-4-ANEPBS, BNBIQ, ANNINE-5, and ANNINE-6 values of 12, 21, 24, 31, and 39 D. The effective displacements of an elementary charge e_0 along the membrane normal $(\Delta\mu_{EG}/e_0)\cos\vartheta$ are 0.24, 0.43, 0.51, 0.65, and 0.81 nm. With respect to charge displacement, ANNINE-6 is better by a factor of 3 than the classical styryl dye RH-421. The enhancement may be due either to a stronger intramolecular charge shift $\Delta\mu_{EG}$ or to a better orientation $\cos\vartheta$ in the membrane. A discrimination of the two effects is not possible on the basis of the present data. It may be achieved by systematic measurements of the chromophore orientation in the neuron membrane and by quantum chemical computations of the electronic structure of the chromophores.

Electrochromism and Membrane Solvatochromism. The assignment of a Stark effect to the electrochromic blue shift is confirmed by a consideration of solvatochromism in the neuron membrane. Because of their orientation, the chromophores at the membrane/water interface are in an extremely inhomogeneous environment that may give rise to specific solvatochromic effects with amphiphilic hemicyanines.[33] We have to distinguish the effect of local polarity and the effect of the local polarity gradient.[34] In homogeneous solvents, changing polarity gives rise to a symmetric opposite shift of excitation and emission spectra with an invariant average wavenumber $\bar{\nu}_{00} = (\bar{\nu}_{ex}^{max} + \bar{\nu}_{em}^{max})/2$ of the 00 energy.[12] As a consequence, a shift $\Delta\bar{\nu}_{00} = \bar{\nu}_{00}^{mem} - \bar{\nu}_{00}$ of the average wavenumber in the membrane may be considered to be a quantitative indicator for an effect of the polarity gradient. The wavenumbers $\bar{\nu}_{00}^{mem}$ in the neuron membrane and the 00 energies $\bar{\nu}_{00}$ in bulk solvents[12,24] are summarized in Table 4. There is indeed a large blue shift for all dyes that increases in the series RH-421, di-4-ANEPBS, BNBIQ, ANNINE-5, and ANNINE-6.

We may expect that the solvatochromic effect of the polarity gradient is related to the intramolecular charge displacement $\Delta\mu_{EG}\cos\vartheta$ across the polarity gradient. Thus, we express the blue shift $\Delta\bar{\nu}_{00}$ by eq 8.

$$hc\Delta\bar{\nu}_{00} = E_0\Delta\mu_{EG}\cos\vartheta \qquad (8)$$

The effective internal electric field E_0 characterizes the strength of the gradient. On the basis of eq 8, the increasing solvatochromic blue shifts $\Delta\bar{\nu}_{00}$ in the series RH-421, di-4-ANEPBS, BNBIQ, ANNINE-5, and ANNINE-6 reflect an increasing charge displacement $\Delta\mu_{EG}\cos\vartheta$. Because electrochromism caused by a Stark effect and solvatochromism induced by a polarity gradient are both proportional to $\Delta\mu_{EG}\cos\vartheta$, we expect a proportionality of the electrochromic shift $\Delta\bar{\nu}_{ex}^{max}$ and the solvatochromic shift $\Delta\bar{\nu}_{00}$. In fact, Figure 7 shows such a linear correlation with $\Delta\bar{\nu}_{ex}^{max} = 0.045\Delta\bar{\nu}_{00}$ and confirms the consistency of our interpretations.

TABLE 4: Membrane Solvatochromism and Electrochromism[a]

	$\bar{\nu}_{00}^{mem}$ [cm^{-1}]	$\bar{\nu}_{00}$ [cm^{-1}]	$\Delta\bar{\nu}_{00}$ [cm^{-1}]	$\Delta\bar{\nu}_{ex}^{max}$ [cm^{-1}]
RH-421	17 833	16 500	1333	47
di-4-ANEPBS	18 795	16 800	1995	90
BNBIQ	19 712	17 200	2512	103
ANNINE-5	20 787	17 900	2888	132
ANNINE-6	20 565	17 400	3165	163

[a] Averages of the maxima of excitation and emission in the neuron membrane $\bar{\nu}_{00}^{mem} = (\bar{\nu}_{ex}^{max} - \bar{\nu}_{em}^{max})/2$, 00 energies $\bar{\nu}_{00}$ in bulk solvents, solvatochromic blue shifts $\Delta\bar{\nu}_{00} = \bar{\nu}_{00}^{mem} - \bar{\nu}_{00}$, and electrochromic blue shifts of excitation $\Delta\bar{\nu}_{ex}^{max}$ for an applied voltage change $\Delta V_M = 100$ mV in the neuron are shown. $\bar{\nu}_{00}$ in bulk solvents are for RH-160 instead of 421 and for di-4-ANEPPS instead of di-4-ANEPBS.

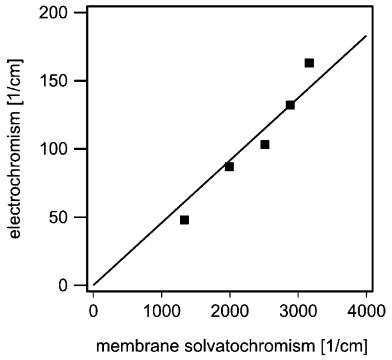

Figure 7. Electrochromism and membrane solvatochromism. Blue shift $\Delta\bar{\nu}_{ex}^{max}$ of the excitation spectra induced by a membrane voltage of $\Delta V_M = 100$ mV versus a shift $\Delta\bar{\nu}_{00} = \bar{\nu}_{00}^{mem} - \bar{\nu}_{00}$ of the average wavenumbers of excitation and emission $\bar{\nu}_{00}^{mem} = (\bar{\nu}_{ex}^{max} - \bar{\nu}_{em}^{max})/2$ in the membrane with respect to the 00 energy $\bar{\nu}_{00}$ in bulk solvents. The dots refer to dyes 1−5 in Figure 1. The linear regression line has a slope of 0.045.

Ideal Stark-Effect Probes. A molecular Stark effect may affect not only the excitation but also the emission of a dye. The resulting spectral shift is described by eq 9.

$$hc\Delta\bar{\nu}_{em}^{max} = \Delta\mu_{EG}\Delta E\cos\vartheta \qquad (9)$$

In fact, for BNBIQ, ANNINE-5, and ANNINE-6, we observe electrochromic blue shifts of emission that are almost identical to those of excitation (Table 3). We assign that correspondence to an identical molecular Stark effect for excitation and emission with an identical charge shift $\Delta\mu_{EG}\cos\vartheta$ due to an identical electronic transition and a similar orientation of the chromophore for excitation and emission.

To determine how far the Stark effect of excitation and emission dominates the voltage sensitivity of BNBIQ, ANNINE-5, and ANNINE-6, we compute the sensitivity spectrum $S_V(\bar{\nu}_{ex},\bar{\nu}_{em})$ for an identical blue shift of excitation and emission at invariant spectral shape and amplitude with $\Delta W_{ex} = \Delta W_{em} = \Delta b_{ex} = \Delta b_{em} = \Delta F_{\bar{\nu}}^{max} = 0$ using eqs 4 and 5.

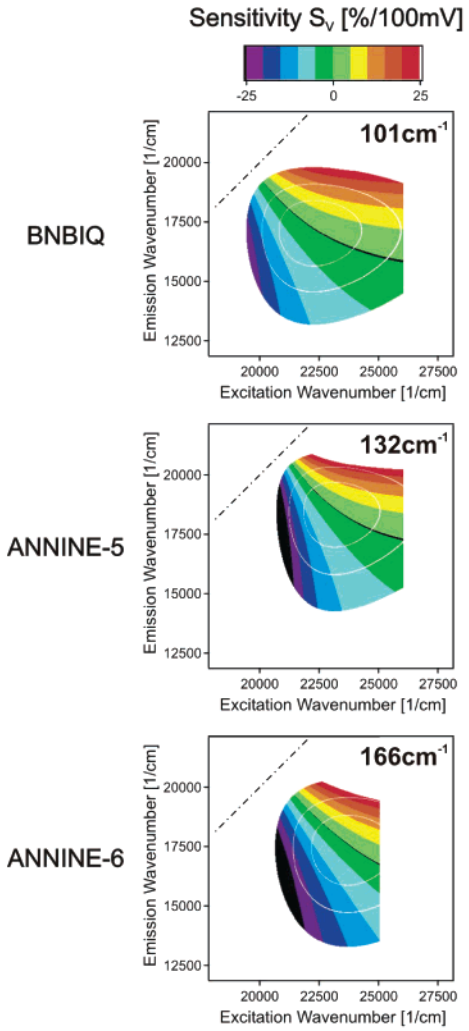

Figure 8. Voltage sensitivity for the molecular Stark effect. Color-coded sensitivity spectra $S_V(\bar{\nu}_{ex},\bar{\nu}_{em}) = \Delta F_{\bar{\nu}}/F_{\bar{\nu}}\Delta V_M$ in the range of relative intensity $F_{\bar{\nu}}/F_{\bar{\nu}}^{max} > 0.1$ where the S_0/S_2 transition plays a negligible role. The spectral shifts of excitation and emission by a voltage change of $\Delta V_M = 100$ mV are $\Delta\bar{\nu}_{ex,em} = 101$ cm^{-1} for BNBIQ, $\Delta\bar{\nu}_{ex,em} = 132$ cm^{-1} for ANNINE-5, and $\Delta\bar{\nu}_{ex,em} = 166$ cm^{-1} for ANNINE-6. The diagonals mark equal wavenumbers of excitation and emission. White lines in the sensitivity and response spectra indicate intensity levels $F_{\bar{\nu}}/F_{\bar{\nu}}^{max} = 0.33$ and $F_{\bar{\nu}}/F_{\bar{\nu}}^{max} = 0.67$. Black lines mark the change in sign of sensitivity and response.

Choosing the averages $\Delta\bar{\nu}_{ex,em}^{max} = (\Delta\bar{\nu}_{ex}^{max} + \Delta\bar{\nu}_{em}^{max})/2$ of the blue shifts from Table 2, we obtain Figure 8. The computed voltage sensitivities are most similar to the fitted spectra in the central column of Figure 5: BNBIQ, ANNINE-5, and ANNINE-6 are almost ideal Stark probes for voltage changes in nerve cells.

When we express the voltage sensitivity for a pure Stark effect by eq 6, considering a small spectral shift $\Delta\bar{\nu}_{ex,em}$, we obtain eq 10 in terms of the derivatives of the absorption and emission spectra $\epsilon' = d\epsilon/d\nu_{ex}$ and $f' = df/d\bar{\nu}_{em}$.

$$S_V(\bar{\nu}_{ex},\bar{\nu}_{em}) = \frac{\Delta\bar{\nu}_{ex,em}}{\Delta V_M}\left[\frac{\epsilon'(\bar{\nu}_{ex})}{\epsilon(\bar{\nu}_{ex})} + \frac{f_{\bar{\nu}}'(\bar{\nu}_{em})}{f_{\bar{\nu}}(\bar{\nu}_{em})}\right] \qquad (10)$$

The voltage sensitivity $S_V(\bar{\nu}_{ex},\bar{\nu}_{em})$ depends not only on the spectral shift caused by the intramolecular charge displacement but also on the shapes of the absorption and emission spectra that are determined by the Franck−Condon factors of the vibroelectronic transitions. The relative slope of the excitation spectrum for ANNINE-5 and ANNINE-6 is highest and positive in the red, whereas the relative slope of the emission spectrum is highest and negative in the blue, as shown in Figures 5 and 6. The relative slopes are distinctly smaller in the blue of excitation and in the red of emission. However, because of their different signs, optimal sensitivitites with respect to excitation and emission cannot be combined. For optical recording, we may choose the red corner of the 2D sensitivity spectra as illustrated in Figure 5. In accordance with eq 10, the sensitivity increases dramatically in the red of excitation but only modestly in the red of emission, as illustrated also by the 1D spectra of Figure 6.

Styryl Dyes. For styryl dyes di-4-ANEPBS and RH421, the spectral shifts of excitation and emission are not identical (Table 2). The blue shift of emission for di-4-ANEPBS is about 50% of the blue shift of excitation, and RH-421 even exhibits a red shift of emission. These results do not depend on the fitting procedure (Table 3). Apparently, with these dyes, the emission is affected by other effects besides a Stark effect. Possibly, the electrical field changes the position and orientation of the excited chromophores, resulting in a field-induced solvatochromic red shift of emission that is superimposed on a Stark effect.

Optical Recording. The sensitivity function $S_V(\bar{\nu}_{ex},\bar{\nu}_{em})$ reflects molecular features of the membrane-bound dye according to eq 6. However, the photodiode signal $\Delta P(\bar{\nu}_{ex},\bar{\nu}_{em})$ due to a voltage change ΔV_M of neuronal activity in an experimental setup of optical recording depends not only on voltage sensitivity but also on staining, illumination, and detection.[35,36] Considering eqs 1 and 2, we obtain eq 11: a high response requires a large observed membrane area A_{mem}, a high density of dye molecules per unit area n_{dye}, a high quantum intensity of illumination $I\bar{\nu}^{ill}(\bar{\nu}_{ex})\Delta\bar{\nu}_{ex}$, a high efficiency of the detection system $T^{rec}(\bar{\nu}_{em})\Delta\bar{\nu}_{em}$, a high voltage sensitivity $S_V(\bar{\nu}_{ex},\bar{\nu}_{em})$ and, considering $F_{\bar{\nu}}(\bar{\nu}_{ex},\bar{\nu}_{em}) = \epsilon(\bar{\nu}_{ex})\, f_{\bar{\nu}}(\bar{\nu}_{em})\Phi_{em}$, a high cross section of absorption $\epsilon(\bar{\nu}_{ex})$ and a high yield of fluorescence $f_{\bar{\nu}}(\bar{\nu}_{em})\Phi_{em}$.

$$\Delta P(\bar{\nu}_{ex},\bar{\nu}_{em}) = \Delta V_M A_{mem} n_{dye} \cdot I_{\bar{\nu}}^{ill}(\bar{\nu}_{ex})\Delta\bar{\nu}_{ex} \cdot S_V(\bar{\nu}_{ex},\bar{\nu}_{em}) \cdot F_{\bar{\nu}}(\bar{\nu}_{ex},\bar{\nu}_{em}) \cdot T^{rec}(\bar{\nu}_{em})\Delta\bar{\nu}_{em} \qquad (11)$$

We consider an illumination with a narrow spectral bandwidth at a wavenumber $\bar{\nu}_{ex}^*$ with an integral intensity $I^{ill} = \int I\bar{\nu}^{ill}(\bar{\nu}_{ex})\, d\bar{\nu}_{ex}$ and a detection with constant efficiency $T^{rec}(\bar{\nu}_{em}) = T^{rec}$ within the spectral limits $\bar{\nu}_{em}^A$ and $\bar{\nu}_{em}^B$ of recording. The total photodiode signal is given by eq 12.

$$\Delta P = \Delta V_M A_{mem} n_{dye} I^{ill} T^{rec} \int_{\bar{\nu}_{em}^A}^{\bar{\nu}_{em}^B} F_{\bar{\nu}}(\bar{\nu}_{ex}^*,\bar{\nu}_{em})\, S_V(\bar{\nu}_{ex}^*,\bar{\nu}_{em})\, d\bar{\nu}_{em} \qquad (12)$$

An optimal signal is achieved by good staining, high illumination intensity, high detector sensitivity, and the proper selection of the excitation wavenumber $\bar{\nu}_{ex}^*$ and the emission filters $\bar{\nu}_{em}^A$ and $\bar{\nu}_{em}^B$ to attain a large integral over the product of the sensitivity spectrum and the fluorescence spectrum. For illustration, the normalized response spectrum $R_V(\bar{\nu}_{ex},\bar{\nu}_{em}) = S_V(\bar{\nu}_{ex},\bar{\nu}_{em})F_{\bar{\nu}}(\bar{\nu}_{ex},\bar{\nu}_{em})/F_{\bar{\nu}}^{max}$ is plotted in the right column of Figure 5. The highest negative integrals are found in the red corner of the spectrum with an excitation wavenumber $\bar{\nu}_{ex}^*$ at the minimum of $R_V(\bar{\nu}_{ex},\bar{\nu}_{em})$ and with emission filters $\bar{\nu}_{em}^A$ and $\bar{\nu}_{em}^B$ excluding the region of positive response. The

highest reponse increases significantly in the series RH-421, di-4-ANEPBS, BNBIQ, ANNINE-5, and ANNINE-6.

Signal-to-Noise Ratio. The total response expressed by eq 12 reflects the signal-to-noise ratio only if the noise is constant (e.g., dominated by the electronic amplifier). If the shot noise of photons dominates,[37] then we have to consider a noise level $N = \sqrt{P/2\tau_D}$ that depends on the total photon count P and the time constant of the detector τ_D. With

$$P = A_{mem} n_{dye} I^{ill} T^{rec} \int_{\bar{\nu}_{em}^A}^{\bar{\nu}_{em}^B} F_{\bar{\nu}}(\bar{\nu}_{ex}^*, \bar{\nu}_{em})\, d\bar{\nu}_{em}$$

we obtain eq 13.

$$\frac{\Delta P}{N} = \Delta V_M \sqrt{2\tau_D A_{mem} I^{ill} n_{dye} T^{rec} \Phi_{em}} \times \frac{\int_{\bar{\nu}_{em}^A}^{\bar{\nu}_{em}^B} F_{\bar{\nu}}(\bar{\nu}_{ex}^*, \bar{\nu}_{em})\, S_{\bar{\nu}}(\bar{\nu}_{ex}^*, \bar{\nu}_{em})\, d\bar{\nu}_{em}}{\sqrt{\int_{\bar{\nu}_{em}^A}^{\bar{\nu}_{em}^B} F_{\bar{\nu}}(\bar{\nu}_{ex}^*, \bar{\nu}_{em})\, d\bar{\nu}_{em}}} \quad (13)$$

In optimizing the signal-to-noise ratio, we have to take into account the roles of photobleaching and phototoxicity of the dyes. These effects impair optical recording because dyes and cells fade away by illumination. Both photochemical processes are determined by the number of excitations per unit time. The signal-to-noise ratio must be optimized with the constraint of a certain number of excitations per unit time that is tolerable for a certain experiment. When we express the fluorescence spectrum by $F_{\bar{\nu}}(\bar{\nu}_{ex}^*, \bar{\nu}_{em}) = \epsilon(\bar{\nu}_{ex}^*)\Phi_{em} f_{\bar{\nu}}(\bar{\nu}_{em})$, we obtain eq 14.

$$\frac{\Delta P}{N} = \Delta V_M \sqrt{2\tau_D A_{mem}} \sqrt{I^{ill} n_{dye} \epsilon(\bar{\nu}_{ex}^*)} \sqrt{T^{rec} \Phi_{em}} \times \frac{\int_{\bar{\nu}_{em}^A}^{\bar{\nu}_{em}^B} f_{\bar{\nu}}(\bar{\nu}_{em})\, S_{\bar{\nu}}(\bar{\nu}_{ex}^*, \bar{\nu}_{em})\, d\bar{\nu}_{em}}{\sqrt{\int_{\bar{\nu}_{em}^A}^{\bar{\nu}_{em}^B} f_{\bar{\nu}}(\bar{\nu}_{em})\, d\bar{\nu}_{em}}} \quad (14)$$

Here the signal-to-noise ratio is expressed in terms of (i) the spatio-temporal resolution $\tau_D A_{mem}$ of the setup, (ii) the number of excitations per area and time $I^{ill} n_{dye} \epsilon(\bar{\nu}_{ex}^*)$, (iii) the yield of detected quanta $T^{rec}\Phi_{em}$, and (iv) the sensitivity function $S_{\bar{\nu}}(\bar{\nu}_{ex}^*, \bar{\nu}_{em})$ weighted by the fluorescence spectrum $f_{\bar{\nu}}(\bar{\nu}_{em})$ within the spectral limits of detection. With the constraint $I^{ill}\epsilon(\bar{\nu}_{ex}^*) = \text{const}$, the choice of an optimal wavenumber of excitation $\bar{\nu}_{ex}^*$ and the choice of optimal emission filters $\bar{\nu}_{em}^A$ and $\bar{\nu}_{em}^B$ are determined by a weighted sensitivity function $\langle S_V(\bar{\nu}_{ex}^*)\rangle$, defined by eq 15.

$$\langle S_V(\bar{\nu}_{ex}^*)\rangle = \frac{\int_{\bar{\nu}_{em}^A}^{\bar{\nu}_{em}^B} f_{\bar{\nu}}(\bar{\nu}_{em})\, S_{\bar{\nu}}(\bar{\nu}_{ex}^*, \bar{\nu}_{em})\, d\bar{\nu}_{em}}{\sqrt{\int_{\bar{\nu}_{em}^A}^{\bar{\nu}_{em}^B} f_{\bar{\nu}}(\bar{\nu}_{em})\, d\bar{\nu}_{em}}} \quad (15)$$

For the ANNINE dyes, the sensitivity $S_{\bar{\nu}}(\bar{\nu}_{ex}^*, \bar{\nu}_{em})$ (Figure 5) reaches its largest negative values in the red corner of the spectrum. We expect a high signal-to-noise ratio when we excite monochromatically at a rather low wavenumber $\bar{\nu}_{ex}^*$. To keep $I^{ill}\epsilon(\bar{\nu}_{ex}^*)$ constant, we have to compensate the low cross section of absorption by an enhanced illumination intensity. Of course, we have to limit the detection to the range of negative response. For illustration, the weighted sensitivity function $\langle S_V(\bar{\nu}_{ex}^*)\rangle$ obtained from the data is plotted in Figure 9 for ANNINE-6 versus the wavenumber of illumination.

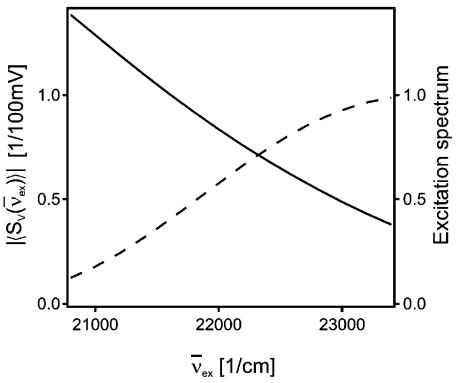

Figure 9. Weighted voltage sensitivity $|\langle S_V(\bar{\nu}_{ex})\rangle|$ of ANNINE-6 versus wavenumber of monochromatic excitation (—) $\bar{\nu}_{ex}$. $|\langle S_V(\bar{\nu}_{ex})\rangle|$ is proportional to the signal-to-noise ratio with the constraint of a constant number of excitation processes per unit time. The detection ranges from 12 000 to 17 600 cm^{-1}. For comparison, the relative excitation spectrum is plotted (– –).

These features of the signal-to-noise ratio for $I^{ill}\epsilon(\bar{\nu}_{ex}^*) = \text{const}$ are expected for a Stark effect. When we insert eq 10 into eq 15, we obtain eq 16.

$$\langle S_V(\bar{\nu}_{ex}^*)\rangle = \frac{\Delta\bar{\nu}_{ex,em}}{\Delta V_M} \sqrt{\int_{\bar{\nu}_{em}^A}^{\nu_{em}^B} f_{\bar{\nu}}(\bar{\nu}_{em})\, d\bar{\nu}_{em}} \times \left\{ \frac{\epsilon'(\bar{\nu}_{ex}^*)}{\epsilon(\bar{\nu}_{ex}^*)} + \frac{\int_{\bar{\nu}_{em}^A}^{\bar{\nu}_{em}^B} f_{\bar{\nu}}'(\bar{\nu}_{em})\, d\bar{\nu}_{em}}{\int_{\bar{\nu}_{em}^A}^{\bar{\nu}_{em}^B} f_{\bar{\nu}}(\bar{\nu}_{em})\, d\bar{\nu}_{em}} \right\} \quad (16)$$

When we choose an excitation wavenumber in the red where the relative slope of the excitation spectrum is steep, we expect an increasing contribution of the Stark effect of excitation at a rather invariant contribution of the Stark effect of emission. Thus, we expect an increasing signal-to-noise ratio for an illumination $\bar{\nu}_{ex}^*$ at the red end of the excitation spectrum. Of course, the signal-to-noise ratio is proportional to the spectral shift by the Stark effect.

Conclusions

Anellated hemicyanine dyes ANNINE-5 and ANNINE-6 exhibit voltage sensitivities in a neuron membrane that are distinctly higher than those of the classical styryl dyes. These novel probes rely on a well-defined physical mechanism, the molecular Stark effect. Their excellence in the optical recording of neuronal excitation is due to a large intramolecular charge shift in connection with suitable Franck−Condon factors of vibroelectronic transitions and a high quantum yield of fluorescence. Further improvements to the voltage-sensitive dyes must be directed toward higher photochemical stability and lower phototoxicity and toward the selective staining of individual cells in a tissue.

Acknowledgment. We thank Gerd Hübener, Birgit Haringer, and Michaela Morawetz for the synthesis of the dyes, Armin Lambacher for discussions, and Marlon Hinner and Armin Lambacher for critically reading the manuscript. This project was supported in part by the Fonds der Chemischen Industrie.

References and Notes

(1) Bullen, A.; Saggau, P. Optical Recording from Individual Neurons in Culture. In *Modern Techniques in Neuroscience Research*, 1st ed.; Johansson, H., Ed.; Springer-Verlag: Berlin, 1999; p 89.

(2) Sinha, S. R.; Saggau, P. Optical Recording from Populations of Neurons in Brain Slices. In *Modern Techniques in Neuroscience Research*, 1st ed.; Johansson, H., Ed.; Springer-Verlag: Berlin, 1999; p 459.
(3) Grinvald, A.; Shoham, D.; Shmuel, A.; Glaser, D.; Vanzetta, I.; Shtoyerman, E.; Slovin, H.; Wijnbergen, C.; Hildesheim, R.; Arieli, A. In-Vivo Optical Imaging of Cortical Architecture and Dynamics. In *Modern Techniques in Neuroscience Research*, 1st ed.; Johansson, H., Ed.; Springer-Verlag: Berlin, 1999; p 893.
(4) Tasaki, I.; Watanabe, A.; Sandlin, R.; Carnay, L. *Proc. Natl. Acad. Sci. U.S.A.* **1968**, *61*, 883.
(5) Cohen, L. B.; Salzberg, B. M.; Davila, H. V.; Ross, W. N.; Landowne, D.; Waggoner, A. S.; Wang, C. H. *J. Membr. Biol.* **1974**, *19*, 1.
(6) Cohen, L. B.; Salzberg, B. M. *Rev. Physiol. Biochem. Pharmacol.* **1978**, *83*, 35.
(7) Loew, L. M.; Bonneville, G. W.; Surow, J. *Biochemistry* **1978**, *17*, 4065.
(8) Loew, L. M.; Simpson, L. L. *Biophys. J.* **1981**, *34*, 353.
(9) Fluhler, E.; Burnham, V. G.; Loew, L. M. *Biochemistry* **1985**, *24*, 5749.
(10) Grinvald, A.; Hildesheim, R.; Farber, I. C.; Anglister, L. *Biophys. J.* **1982**, *39*, 301.
(11) Grinvald, A.; Fine, A.; Farber, I. C.; Hildesheim, R. *Biophys. J.* **1983**, *42*, 195.
(12) Fromherz, P. *J. Phys. Chem.* **1995**, *99*, 7188.
(13) Fromherz, P.; Lambacher, A. *Biochim. Biophys. Acta* **1991**, *1068*, 149.
(14) Fromherz, P.; Muller, C. O. *Biochim. Biophys. Acta* **1993**, *1150*, 111.
(15) Loew, L. M.; Cohen, L. B.; Salzberg, B. M.; Obaid, A. L.; Venzanilla, F. *Biophys. J.* **1985**, *47*, 7.
(16) Fromherz. P.; Dambacher, K. H.; Ephardt, H.; Lambacher, A.; Muller, C. O.; Neigl, R.; Schaden, H.; Schenk, O.; Vetter, T. *Ber. Bunsen-Ges. Phys. Chem.* **1991**, *95*, 1333.
(17) Ephardt, H.; Fromherz, P. *J. Phys. Chem.* **1989**, *93*, 7717.
(18) Rocker, C.; Heilemann, A.; Fromherz, P. *J. Phys. Chem.* **1996**, *100*, 12172.
(19) Fromherz, P.; Rocker, C. *Ber. Bunsen-Ges. Phys. Chem.* **1994**, *98*, 128.
(20) Visser, N. V.; van Hoek, A.; Visser, A. J.; Frank, J.; Apell, H. J.; Clarke, R. J. *Biochemistry* **1995**, *34*, 11777.
(21) Lambacher, A.; Fromherz, P. *J. Phys. Chem. B* **2001**, *105*, 343.
(22) Gupta, R. K.; Salzberg, B. M.; Grinvald, A.; Cohen, L. B.; Kamino, K.; Lesher, S.; Boyle, M. B.; Waggoner, A. S.; Wang, C. H. *J. Membr. Biol.* **1981**, *58*, 123.
(23) Ephardt, H.; Fromherz, P. *J. Phys. Chem.* **1993**, *97*, 4540.
(24) Huebener, G.; Lambacher, A.; Fromherz, P. *J. Phys. Chem. B* **2003**, *107*, 7896.
(25) Dietzel, I. D.; Drapeau, P.; Nicholls, J. G. *J. Physiol. (London)* **1986**, *372*, 191.
(26) Meyer, E.; Muller, C. O.; Fromherz, P. *Eur. J. Neurosci.* **1997**, *9*, 778.
(27) Hamill, O. P.; Marty, A.; Neher, E.; Sakmann, B.; Sigworth, F. J. *Pfluegers Arch.* **1981**, *391*, 85.
(28) Siano, D. B.; Metzler, D. E. *J. Chem. Phys.* **1969**, *51*, 1856.
(29) Junge, W.; Witt, H. T. *Z. Naturforsch., B* **1968**, *23*, 244.
(30) Bucher, H.; Wiegand, J.; Snavely, B. B.; Beck, K. H.; Kuhn, H. *Chem. Phys. Lett.* **1969**, *3*, 508.
(31) Reich, R.; Schmidt, S. *Ber. Bunsen-Ges. Phys. Chem.* **1972**, *76*, 589.
(32) Schmidt, S.; Reich, R. *Ber. Bunsen-Ges. Phys. Chem.* **1972**, *76*, 1202.
(33) Loew, L. M.; Simpson, L.; Hassner, A.; Alexanian, V. *J. Am. Chem. Soc.* **1979**, *101*, 5439.
(34) Ephardt, H.; Fromherz, P. *J. Phys. Chem.* **1991**, *95*, 6792.
(35) Waggoner, A. *J. Membr. Biol.* **1976**, *27*, 317.
(36) Salzberg, B. M. Optical Recording of Electrical Activity in Neurons Using Molecular Probes. In *Current Methods in Cellular Neurobiology*; Barker, J., Ed.; Wiley: New York, 1983; p 139.
(37) Knopfel, T.; Fromherz, P. *Z. Naturforsch., C* **1987**, *42*, 986.